

Magnetorotational supernovae with jets

S.G.Moiseenko^{1*}, G.S.Bisnovatyi-Kogan^{1†} and N.V.Ardeljan^{2‡}

¹*Space Research Institute, Profsoyuznaya str. 84/32, Moscow 117997, Russia*

²*Department of Computational Mathematics and Cybernetics, Moscow State University, Vorobjevy Gory, Moscow B-234, Russia*

Accepted . Received ; in original form

ABSTRACT

We present results of 2D simulation of magnetorotational (MR) supernova accompanied by jet formation in the core collapse supernova explosion. Initial magnetic field used in the simulations has dipole-like symmetry. Contrary to the simulations of MR supernova with initial quadrupole-like magnetic field, where the matter was ejected mainly near the equatorial plane, in presence of the dipole-like initial magnetic field the supernova explosion is developing preferably along a rotational axis, and leads to formation of a protojet. We expect that protojet propagation through the envelope of the star will be accompanied by its collimation. The magnetorotational instability (MRI) was found in simulations, similar to the earlier considered case of the quadrupole-like initial magnetic field. Our estimations show that the characteristic time for the reconnection of the magnetic field is much larger than the MRI development time. The supernova explosion energy for the dipole-like field is about $0.61 \cdot 10^{51}$ erg, and about $0.13M_{\odot}$ of mass was ejected during the explosion.

Key words: MHD-supernovae: general.

1 INTRODUCTION

The idea of the MR mechanism of the core collapse supernova, suggested by Bisnovatyi-Kogan (1970), was to get energy for the supernova explosion from the rotation of the star due to magnetic field action. During the collapse stellar rotation is becoming differential i.e. central parts of the star rotate much faster than the envelope. 1D numerical simulations made by Bisnovatyi-Kogan et al. (1976), Ardelyan et al. (1979) had shown that the differential rotation in presence of magnetic field leads to appearing of the toroidal component of the magnetic field, its linear growth, and following formation of MHD shock wave. In 1D approach the rotation was differential along r axis only (the star in 1D was a cylinder) what means that the only H_r component of the magnetic field was wounded up and produced the toroidal (H_{φ}) component. In a 2D case the system has more degrees of freedom and the rotation is differential not only along the r axis. The differential rotation is using both components of the magnetic field (H_r, H_z) for the toroidal field amplification. 2D simulations of MR mechanism with the initial magnetic field of the quadrupole-like type of symmetry have shown (Ardeljan et al. (2000), Moiseenko et al. (2004), Ardeljan et al. (2005)) that the amplification of the toroidal component of the magnetic field leads to formation

of a compression wave, which moves along steeply decreasing density profile and quickly transforms into the fast MHD shock wave. Due to the quadrupole-like initial magnetic field the supernova explosion was developed predominantly along the equatorial plane. The explosion energy for that case was about $0.6 \cdot 10^{51}$ erg. The value of the ejected energy is enough for the explanation of the core collapse supernova explosion. The main qualitative difference between 1D (Ardelyan et al. (1979)) and 2D (Ardeljan et al. (2005)) MR supernova simulation is an appearance of the magnetorotational instability (MRI) which significantly reduces the time of the growth of the toroidal magnetic field up to MR supernova explosion. In 1D case the MRI is not developed due to the small number of degrees of freedom.

The first simulations of the MR processes in stars have been done by LeBlanc & Wilson 1970, after which MR processes in the stars in relation to the core collapse supernova explosion had been simulated by Bisnovatyi-Kogan et al. 1976, Ardelyan et al. 1979, Müller & Hillebrandt 1979, Ohnishi 1983, Symbalisty 1984. Recently the interest to the MR processes (especially in application to the core collapse supernova) was recommenced due to increasing number of observational data about asymmetry of the explosion, and possible collimated ejecta in connection with cosmic gamma ray bursts (Ardeljan et al. 2000; Akiyama et al. 2003; Yamada & Sawai 2004; Kotake et al. 2004; Kotake et al. 2004; Ardeljan et al. 2005; Yamasaki & Yamada 2005). In the paper by Bisnovatyi-Kogan & Tutukov (2004) it was es-

* E-mail: moiseenko@iki.rssi.ru (SGM)

† gkogan@iki.rssi.ru (GSBK)

‡ ardel@cs.msu.su (NVA)

timated that a significant part of the type Ib,c supernovae could explode as magnetorotational supernovae.

In the present paper we describe the results of the 2D simulations of the MR supernova explosion with the initial dipole-like magnetic field. The qualitative difference between our simulation of the same problem with the initial quadrupole-like magnetic field is the formation of mildly collimated protojet, directed along the rotational axis. As in the paper by Ardeljan et al. (2005) we have found a development of the MRI leading to rapid explosion even at a relatively weak initial magnetic field. In the simulations we have used an ideal MHD with the infinite conductivity. In spite of the fact that we supposed the conductivity to be infinite, in reality it is very big, but finite. That means that during winding up the force lines of the magnetic field and the MRI development, the reconnection of the magnetic field lines is possible. If the reconnection time would be smaller or comparable to the characteristic time of the MRI development then the reconnection process could reduce effectiveness of the MR supernova mechanism.

We have done estimations for the reconnection time and have found that it is much larger than the time of the development of the MRI, and will not influence significantly on the MR supernova explosion. MRI in application to the core collapse supernova was studied by Spruit (2002), Akiyama et al. (2003).

For the simulations we have used implicit Lagrangian numerical method on triangular grid of variable structure. This method was used for the simulations of a number of different astrophysical problems: simulations of the collapse of cold rapidly rotating protostellar clouds (Ardeljan et al. (1996)), magnetorotational processes for the collapsing magnetized protostellar cloud (Ardeljan et al. (2000)), core collapse and formation of the neutron star (Ardeljan et al. (2004)), MR supernova simulations with quadrupole-like initial magnetic field (Ardeljan et al. (2005)).

2 FORMULATION OF THE PROBLEM

2.1 Equations of state and neutrino losses

For the simulations we use the equation of state used in Ardelyan et al. (1987a):

$$P \equiv P(\rho, T) = P_0(\rho) + \rho \mathfrak{R} T + \frac{\sigma T^4}{3},$$

$$P_0(\rho) = \begin{cases} P_0^{(1)} = b_1 \rho^{5/3} / (1 + c_1 \rho^{1/3}), & 0 \leq \rho \leq \rho_1, \\ P_0^{(k)} = a \cdot 10^{b_k (\lg \rho - 8.419)^{c_k}}, & \rho_{k-1} \leq \rho \leq \rho_k, \\ k = 2, 6, \dots \end{cases} \quad (1)$$

$$\begin{aligned} b_1 &= 10^{12.40483} & c_1 &= 10^{-2.257} & \rho_1 &= 10^{9.419} \\ b_2 &= 1. & c_2 &= 1.1598 & \rho_2 &= 10^{11.5519} \\ b_3 &= 2.5032 & c_3 &= 0.356293 & \rho_3 &= 10^{12.26939} \\ b_4 &= 0.70401515 & c_4 &= 2.117802 & \rho_4 &= 10^{14.302} \\ b_5 &= 0.16445926 & c_5 &= 1.237985 & \rho_5 &= 10^{15.0388} \\ b_6 &= 0.86746415 & c_6 &= 1.237985 & \rho_6 &\gg \rho_5 \\ a &= 10^{26.1673}, \end{aligned}$$

where \mathfrak{R} is the gas constant equal to $0.83 \cdot 10^8 \frac{\text{cm}^2}{\text{s}^2} \text{K}$, σ is the constant of the radiation density, P is pressure, ρ is density, and T is temperature. In the expression $P_0(\rho)$ the value ρ

was identified with the total mass-energy density. For the cold degenerated matter expression for $P_0(\rho)$ is the approximation of the tables from Baym et al. (1971); Malone et al. (1975).

In the neighborhood of points $\rho = \rho_k$ in formula (1) the function $P_0(\rho)$ was smoothed in the same way as in Ardelyan et al. (1987a), to make continuous the derivative $dP_0/d\rho$:

$$P_0(\rho) = \begin{cases} P_0^{(k)}, \rho \in [\rho_{k-1} + \xi_{k-1}, \rho_k - \xi_k], \\ k = 1, 6, \rho_0 + \xi_0 = 0, \\ \theta_k P_0^{(k)} + (1 - \theta_k) P_0^{(k+1)}, \\ \rho \in [\rho_k - \xi_k, \rho_k + \xi_k], k = \overline{1, 5}, \end{cases} \quad (2)$$

where

$$\theta_k = \theta(\rho) = \frac{1}{2} - \frac{1}{2} \sin \left(\frac{\pi}{2\xi_k} (\rho - \rho_k) \right), \quad \xi_k = 0.01 \rho_k.$$

The specific energy (per mass unit) was defined thermodynamically as:

$$\varepsilon = \varepsilon_0(\rho) + \frac{3}{2} \mathfrak{R} T + \frac{\sigma T^4}{\rho} + \varepsilon_{Fe}(\rho, T). \quad (3)$$

The value $\varepsilon_0(\rho)$ is defined by the relation

$$\varepsilon_0(\rho) = \int_0^\rho \frac{P_0(\tilde{\rho})}{\tilde{\rho}^2} d\tilde{\rho}. \quad (4)$$

The term ε_{Fe} in equation (3) is responsible for iron dissociation. It is used in the following form:

$$\varepsilon_{Fe}(\rho, T) = \frac{E_{b,Fe}}{A m_p} \left(\frac{T - T_{0Fe}}{T_{1Fe} - T_{0Fe}} \right). \quad (5)$$

It was supposed that in region of the iron dissociation the iron amount was about 50% of the mass, $E_{b,Fe} = 8 \cdot 10^{-5}$ erg is the iron binding energy, $A = 56$ is the iron atomic weight, and $m_p = 1.67 \cdot 10^{-24}$ g is the proton mass, $T_{0Fe} = 0.9 \cdot 10^{10}$ K, $T_{1Fe} = 1.1 \cdot 10^{10}$ K. For the numerical calculations formula (5) has been slightly modified (smoothed):

$$\varepsilon_{Fe}(\rho, T) = \frac{E_{b,Fe}}{A m_p} \frac{\left(1 + \sin \left(\pi \left(\frac{T - T_{0Fe}}{T_{1Fe} - T_{0Fe}} \right) - \frac{\pi}{2} \right) \right)}{2}. \quad (6)$$

The neutrino losses for Urca processes are used in the form, taken from Bisnovatyi-Kogan et al. (1976), approximating the table of Ivanova et al. (1969):

$$f(\rho, T) = \frac{1.3 \cdot 10^9 \mathfrak{a}(\overline{T}) \overline{T}^6}{1 + (7.1 \cdot 10^{-5} \rho \overline{T}^3)^{\frac{2}{5}}} \quad \text{erg} \cdot \text{g}^{-1} \cdot \text{s}^{-1}, \quad (7)$$

$$\mathfrak{a}(\overline{T}) = \begin{cases} 1, & \overline{T} < 7, \\ 664.31 + 51.024(\overline{T} - 20), & 7 \leq \overline{T} \leq 20, \\ 664.31, & \overline{T} > 20, \end{cases} \quad (8)$$

$$\overline{T} = T \cdot 10^{-9}.$$

The neutrino losses from pair annihilation, photo production, and plasma were also taken into account. These types of the neutrino losses have been approximated by the interpolation formulae from Schindler et al. (1987):

$$Q_{tot} = Q_{pair} + Q_{photo} + Q_{plasm}. \quad (9)$$

The three terms in (9) can be written in the following general form:

$$Q_d = K(\rho, \alpha) e^{-c\xi} \frac{a_0 + a_1 \xi + a_2 \xi^2}{\xi^3 + b_1 \alpha + b_2 \alpha^2 + b_3 \alpha^3}. \quad (10)$$

For $d = \text{pair}$, $K(\rho, \alpha) = g(\alpha) e^{-2\alpha}$,

$$g(\alpha) = 1 - \frac{13.04}{\alpha^2} + \frac{133.5}{\alpha^4} + \frac{1534}{\alpha^6} + \frac{918.6}{\alpha^8};$$

For $d = \text{photo}$, $K(\rho, \alpha) = (\rho/\mu_Z) \alpha^{-5}$;

For $d = \text{plasm}$, $K(\rho, \alpha) = (\rho/\mu_Z)^3$;

$$\xi = \left(\frac{\rho/\mu_Z}{10^9} \right)^{1/3} \alpha.$$

Here, $\mu_Z = 2$ is the number of nucleons per electron. Coefficients c , a_i , and b_i for the different losses are given in the Table 1 from Schindler et al. (1987). The general formula for the neutrino losses in a nontransparent star has been written in the form, used by Ardeljan et al. (2004):

$$F(\rho, T) = (f(\rho, T) + Q_{tot}) e^{-\frac{\tau_\nu}{10}}. \quad (11)$$

The multiplier $e^{-\frac{\tau_\nu}{10}}$ in formula (11), where $\tau_\nu = S_\nu n l_\nu$, restricts the neutrino flux for non zero depth to neutrino interaction with matter τ_ν . The cross-section for this interaction S_ν was presented in the form:

$$S_\nu = \frac{10^{-44} T^2}{(0.5965 \cdot 10^{10})^2},$$

the concentration of nucleons is

$$n = \frac{\rho}{m_p}.$$

The characteristic length scale l_ν , which defines the depth for the neutrino absorption, was taken to be equal to the characteristic length of the density variation as:

$$l_\nu = \frac{\rho}{|\nabla \rho|} = \frac{\rho}{((\partial \rho / \partial r)^2 + (\partial \rho / \partial z)^2)^{1/2}}. \quad (12)$$

The value l_ν monotonically decreases when moving to the outward boundary; its maximum is in the center. It approximately determines the depth of the neutrino absorbing matter. The multiplier $1/10$ in the expression $e^{-\tau_\nu \frac{1}{10}}$ was applied because in the degenerate matter of the hot neutron star only some of the nucleons with the energy near Fermi boundary, approximately $1/10$, take part in the neutrino processes.

2.2 Basic equations

Consider a set of magnetohydrodynamical equations with selfgravitation and infinite conductivity:

$$\begin{aligned} \frac{d\mathbf{x}}{dt} &= \mathbf{v}, \\ \frac{d\rho}{dt} + \rho \nabla \cdot \mathbf{v} &= 0, \\ \rho \frac{d\mathbf{v}}{dt} &= -\text{grad} \left(P + \frac{\mathbf{H} \cdot \mathbf{H}}{8\pi} \right) + \frac{\nabla \cdot (\mathbf{H} \otimes \mathbf{H})}{4\pi} - \rho \nabla \Phi, \\ \rho \frac{d}{dt} \left(\frac{\mathbf{H}}{\rho} \right) &= \mathbf{H} \cdot \nabla \mathbf{v}, \quad \Delta \Phi = 4\pi G \rho, \quad (13) \\ \rho \frac{d\varepsilon}{dt} + P \nabla \cdot \mathbf{v} + \rho F(\rho, T) &= 0, \\ P &= P(\rho, T), \quad \varepsilon = \varepsilon(\rho, T), \end{aligned}$$

where $\frac{d}{dt} = \frac{\partial}{\partial t} + \mathbf{v} \cdot \nabla$ is the total time derivative, $\mathbf{x} = (r, \varphi, z)$, $\mathbf{v} = (v_r, v_\varphi, v_z)$ is the velocity vector, ρ is the density, P is the pressure, $\mathbf{H} = (H_r, H_\varphi, H_z)$ is the magnetic field vector, Φ is the gravitational potential, ε is the internal energy, G is gravitational constant, $\mathbf{H} \otimes \mathbf{H}$ is the tensor of rank 2, and $F(\rho, T)$ is the rate of neutrino losses.

r , φ , and z are spatial Lagrangian coordinates, i.e. $r = r(r_0, \varphi_0, z_0, t)$, $\varphi = \varphi(r_0, \varphi_0, z_0, t)$, and $z = z(r_0, \varphi_0, z_0, t)$, where r_0, φ_0, z_0 are the initial coordinates of material points of the matter.

Taking into account symmetry assumptions ($\frac{\partial}{\partial \varphi} = 0$), the divergency of the tensor $\mathbf{H} \otimes \mathbf{H}$ can be presented in the following form:

$$\nabla \cdot (\mathbf{H} \otimes \mathbf{H}) = \begin{pmatrix} \frac{1}{r} \frac{\partial(r H_r H_r)}{\partial r} + \frac{\partial(H_z H_r)}{\partial z} - \frac{1}{r} H_\varphi H_\varphi \\ \frac{1}{r} \frac{\partial(r H_r H_\varphi)}{\partial r} + \frac{\partial(H_z H_\varphi)}{\partial z} + \frac{1}{r} H_\varphi H_r \\ \frac{1}{r} \frac{\partial(r H_r H_z)}{\partial r} + \frac{\partial(H_z H_z)}{\partial z} \end{pmatrix}.$$

Axial symmetry ($\frac{\partial}{\partial \varphi} = 0$, $r \geq 0$) and symmetry to the equatorial plane ($z \geq 0$) are assumed. The problem is solved in the restricted domain. At $t = 0$ the domain is restricted by the rotational axis $r \geq 0$, equatorial plane $z \geq 0$, and outer boundary of the star where the density of the matter is zero, while poloidal components of the magnetic field H_r , and H_z can be non-zero.

We assume axial and equatorial symmetry ($r \geq 0$, $z \geq 0$). At the rotational axis ($r = 0$) the following boundary conditions are defined: $(\nabla \Phi)_r = 0$, $v_r = 0$. At the equatorial plane ($z = 0$) the boundary conditions are: $(\nabla \Phi)_z = 0$, $v_z = 0$. At the outer boundary (boundary with vacuum) the following condition is defined: $P_{\text{outer boundary}} = 0$.

We avoid explicit calculations of the function $\varepsilon_0(\rho)$ in (4), because this term is eliminated from (13) due to adiabatic equality:

$$\rho \frac{d\varepsilon_0}{dt} = -\frac{P_0}{\rho} \frac{d\rho}{dt} = P_0 \nabla \cdot \mathbf{v}, \quad (14)$$

determining the fully degenerate part of EOS. Therefore, defining

$$\begin{aligned} \varepsilon^* &= \frac{3}{2} \Re T + \frac{\sigma T^4}{\rho} + \varepsilon_{Fe}(\rho, T), \\ P^* &= \rho \Re T + \frac{\sigma T^4}{3}. \end{aligned}$$

The equation for the internal energy in (13) can be written in the following form:

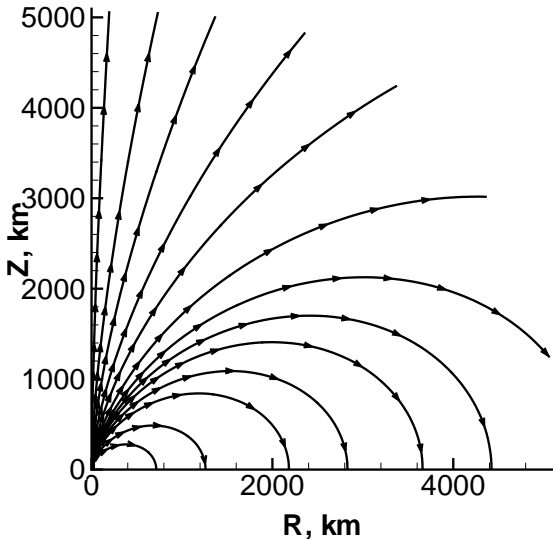
$$\rho \frac{d\varepsilon^*}{dt} + P^* \nabla \cdot \mathbf{v} + \rho F(\rho, T) = 0. \quad (15)$$

2.3 Initial magnetic field

The initial poloidal magnetic field is defined as in our previous papers (Ardeljan et al. (2005), Ardeljan et al. (2000)) by the toroidal current j_φ using Bio-Savara law. The toroidal current which determines the initial magnetic field should be defined in the upper and in the lower hemispheres. The field with the quadrupole-like symmetry is formed by the toroidal current antisymmetrical to the equatorial plane. The dipole-like magnetic field is formed by current symmetrical to the equatorial plane. To define the initial poloidal magnetic field we have used the following toroidal current j_φ (in nondimensional variables):

Table 1. Coefficients for formula (10) from Schindler et al. (1987).

	a_0	a_1	a_2	b_1	b_2	b_3	c
$10^8 \text{ K} \leq T \leq 10^{10} \text{ K}$							
pair	5.026(19)	1.745(20)	1.568(21)	9.383(-1)	-4.141(-1)	5.829(-2)	5.5924
photo	3.897(10)	5.906(10)	4.693(10)	6.290(-3)	7.483(-3)	3.061(-4)	1.5654
plasm	2.146(-7)	7.814(-8)	1.653(-8)	2.581(-2)	1.734(-2)	6.990(-4)	0.56457
$10^{10} \text{ K} \leq T \leq 10^{11} \text{ K}$							
pair	5.026(19)	1.745(20)	1.568(21)	1.2383	-8.1141(-1)	0.0	4.9924
photo	3.897(10)	5.906(10)	4.693(10)	6.290(-3)	7.483(-3)	3.061(-4)	1.5654
plasm	2.146(-7)	7.814(-8)	1.653(-8)	2.581(-2)	1.734(-2)	6.990(-4)	0.56457

**Figure 1.** The initial poloidal dipole-like magnetic field configuration.

$$j_\varphi = \begin{cases} j_\varphi^u & \text{for } z >, < 0; (r - 0.15)^2 + 0.2(z)^2 \leq 0.3^2, \\ 0 & \text{for } (r - 0.15)^2 + 0.2(z)^2 > 0.3^2, \end{cases} \quad (16)$$

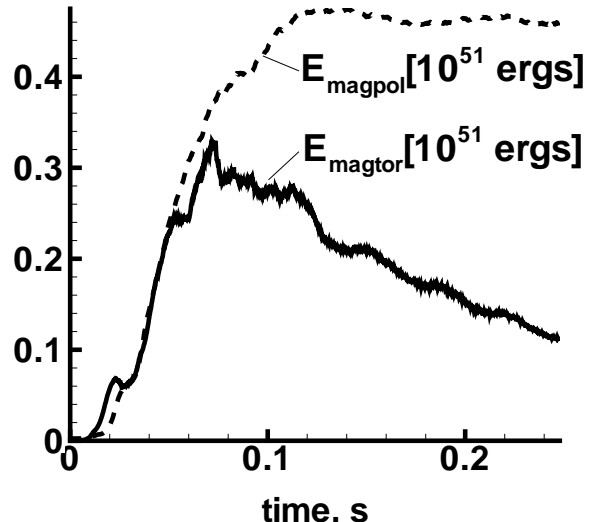
where

$$j_\varphi^u = A_j \times \cos \left[\frac{\pi}{2} \left(\frac{(r - 0.15)^2 + 0.2z^2}{0.3^2} \right) \right]$$

$$j_\varphi^d = j_\varphi^u.$$

The coefficient A_j serves for adjusting the initial magnetic energy. In the dipole-like type of symmetry (16) there is $H_r = 0$ at the equatorial plane ($z = 0$) (Fig. 1). It is important to have a force-free or a balanced initial magnetic field. Using of the nonbalanced initial magnetic field leads to appearance of artificial flows due to "turning on" effect. We start the simulation of the MagnetoRotational Explosion (MRE) from the "equilibrium" state to avoid numerical problems, arising from the nonstationarity, especially in outer region of the core. These regions give a small input into the total energy balance of the explosion.

To construct a configuration, where magnetic forces are balanced with other forces (i.e. gravitational force, gradient of gas pressure and centrifugal force) we follow the procedure from Ardeljan et al. (2000) and Ardeljan et al. (2005). The

**Figure 2.** Time evolution of the toroidal (solid line) and poloidal (dashed line) parts of magnetic energy during MR explosion with dipole-like initial magnetic field.

ratio between the initial magnetic and gravitational energies was chosen to be equal to 10^{-6} , like in Ardeljan et al. (2005), for better comparison of the present results with the results of simulations of MR explosion with the initial quadrupole-like magnetic field. The initial poloidal magnetic field in the center of the star at start of the evolution of the toroidal magnetic field is $\sim 10^{13}$ G.

2.4 Core collapse simulation

For the simulations of the magnetorotational supernova with initial dipole-like magnetic field we first made simulation of the rotating nonmagnetized core collapse Ardeljan et al. (2004). Initially the ratios between the rotational and gravitational energies and between the internal and gravitational energies of the star are the following:

$$\frac{E_{rot}}{E_{grav}} = 0.0057, \quad \frac{E_{int}}{E_{grav}} = 0.727.$$

The rotating core collapse resulted in formation of the proto neutron star and envelope. The bounce shock which was formed during the collapse, goes through the envelope

lope. At the end of calculations in Ardeljan et al. (2004) at $t = 0.2565$ s the bounce shock reaches the outer boundary of our computational domain. The shock leads to the ejection of 0.041 per cent of the core mass and 0.0012 per cent (2.960×10^{48} erg) of the gravitational energy of the star. The amounts of the ejected mass and energy are too small to explain the core collapse supernova explosion. After the core collapse ($t = 0.261$ s) we obtain a differentially rotating configuration. The proto neutron star situated in the center with radius of ~ 12.8 km rotates with the average rotational period 0.00152 s. The angular velocity steeply decreases with the moving from the star center. The particles of the matter situated at the outer boundary in the equatorial plane rotate with the period ~ 35 s due to significant expansion of the envelope after the collapse of the core.

As in previous simulation of the MR explosion with the initial quadrupole-like magnetic field, in the case of the initial dipole-like magnetic field we divide the whole process into three separate parts. The first part is the simulation of the core collapse. The second part is the construction of the balanced star with the dipole-like magnetic field. The third part is the amplification of the toroidal component of the magnetic field H_φ , and MR supernova explosion.

The simulations of the core collapse problem of rotating nonmagnetized core and formation of the proto neutron star and the envelope were described in detail in Ardeljan et al. (2004). We consider the configuration obtained after the core collapse as the initial condition for the simulations.

After the core collapse and formation of a steady state differentially rotating configuration, the initial poloidal magnetic field, defined by the toroidal current (16) was 'turned on'. As in the paper by Ardeljan et al. (2005), at second step the toroidal component was switched off, to obtain a balanced magnetized configuration, and the evolution of only poloidal components (H_r, H_z) of the magnetic field was permitted.

3 NUMERICAL METHOD

The numerical method used in present simulations is based on the implicit operator-difference completely conservative scheme on the Lagrangian triangular grid of variable structure. The implicitness of the applied numerical scheme allows to make large time steps. It is important to use implicit scheme in such kind of problems due to the presence of two strongly different timescales. The small timescale is defined by the huge sound velocity in the central parts of the star. The big time scale is defined by the characteristic timescale of the evolution of the magnetic field. Conservation properties of the numerical scheme are important for the exact fulfillment of the energy balance and divergence-free property of the magnetic field.

During the simulation of the MRE the time step for the implicit scheme was $\sim 10 \div 300$ times larger than time step for the explicit scheme (CFL stability condition). It means that the total number of time steps is $10 \div 300$ times less than it would have been done for explicit scheme, what allows us to decrease time approximation error. We did not make direct comparison of CPU time per time step for our implicit scheme and an explicit scheme. Our estimations show that the total number of arithmetic operations for the implicit

scheme is ≈ 20 times larger than it is required for explicit scheme.

Grid reconstruction procedure applied here for the reconstruction of the triangular lagrangian grid is used both for the correction of the "quality" of the grid and for the dynamical adaptation of the grid.

The method applied here was developed and its stability was investigated in the papers by Ardeljan & Kosmachevskii (1995), Ardeljan et al. (1987) and references therein. It was tested thoroughly with different tests (Ardeljan et al. (2000)).

4 RESULTS

4.1 Magnetorotational supernova explosion and protojet formation

After the core collapse, which does not produce supernova explosion (see section about core collapse simulation), we get a steady state differentially rotating configuration with the rotational period of the central part of the proto neutron star equal to 0.0015 s, and almost rigidly rotating central core of the proto neutron star with the radius ~ 10 km.

The density at the center of the proto neutron star is $\approx 2.4 \times 10^{14}$ g cm $^{-3}$. The ratio of the rotational energy and gravitational energy is ~ 0.073 . The star remains in such a state pretty long time. We have done about 10000 time steps (it corresponds to 0.03s of physical time) and did not notice any significant changes of the parameters of the star. While the inclusion of even weak initial poloidal magnetic field leads to the drastic changes.

After formation of the balanced configuration with the poloidal dipole-like magnetic field, at the moment of 'switching on' the equation for the evolution of the toroidal magnetic field we start counting the time anew.

The toroidal magnetic field component appearing due to the differential rotation is amplifying with time. The fastest amplification of the H_φ takes place in the regions of the maximum of the value $rH \cdot \text{grad}(V_\varphi/r)$ in the equation of the evolution of H_φ . At the initial stage H_φ grows linearly with time (correspondingly toroidal magnetic energy $H_\varphi^2/(8\pi)$ grows as a quadratic function) (Fig.2). Due to appearance of the MRI (which will be described in the following section), after the stage of a linear growth, the toroidal magnetic field starts to grow much faster (exponentially). At this stage the poloidal magnetic field also begins the exponential growth.

The toroidal magnetic energy reaches its maximal value $\approx 3.2 \times 10^{50}$ erg at $t = 0.07$ s. This value is $\approx 66\%$ of the maximal value of the toroidal energy in the case of initial quadrupole-like magnetic field, where this maximum was reached at $t = 0.12$ s (Ardeljan et al. (2005)). The maximal values of the toroidal magnetic field $H_\varphi \approx 1.8 \cdot 10^{16}$ G (in the case of the quadrupole this maximal value was $\sim 2.5 \times 10^{16}$ G) are reached at the distance ~ 10 km from the center of the star.

After reaching its maximal value the toroidal magnetic energy decreases with the time. At the developed stage the poloidal magnetic energy reaches $\approx 4.5 \times 10^{50}$ erg, and does not show any substantial decrease with time.

At $t = 0.07$ s a compression wave appears moving from the central parts of the star due to increasing of the magnetic

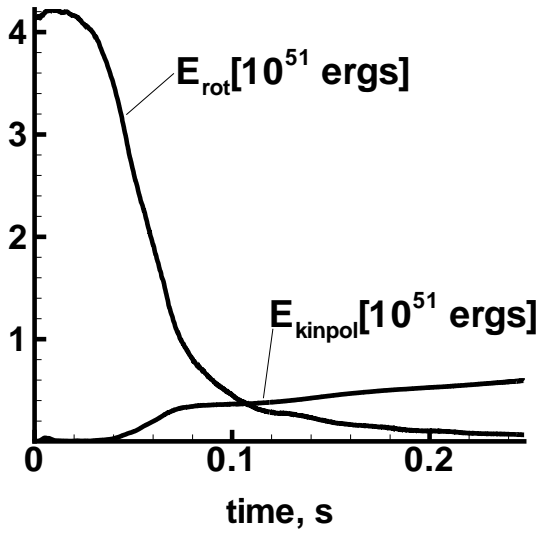


Figure 3. Time evolution of the rotational and radial kinetic energy during MR explosion.

pressure. Moving along a steep density profile the compression wave transforms into the fast MHD shock wave. The development of the MHD shock outwards leads to the ejection of mass and energy.

During the MR explosion a part of the rotational energy ($\approx 10\%$) is transforming into the radial kinetic energy (which could be related to supernova explosion energy). The neutrino transport effects are taken into account approximately in flux limited approximation variant (see section 2.1). A larger fraction of the rotational energy is lost by neutrino emission, while most part of the angular momentum is carried away by the ejected matter.

At the Fig.3 the time evolution of the rotational and radial (poloidal) energies is represented. At the final stage of the MR supernova explosion simulations, the excitation of eigenmodes of the proto neutron star happens. The plot of the radial kinetic energy (Fig. 4) shows that this eigenmode has a period of ≈ 1 ms.

At the Fig. 5 the kinetic energy of the core is represented. This plot was made by subtracting the kinetic energy of the matter expanding by the supernova shock from the total kinetic energy of the star. The amplitude of the kinetic energy of the core oscillations is $\approx 1.3 \cdot 10^{48}$ ergs. In the paper by Burrows et al. (2006) a mechanism of core-collapse supernova explosions was suggested, based on the acoustic energy extracted from the core.

Our simulations have shown that the amount of the acoustic energy generated in the collapsing core is much less than the expected energy of core collapse supernova, note that our mathematical method was different, and we have used more simplified description of the physical processes than Burrows et al. (2006)

At the Figs.6, 7 the time evolution of the neutrino luminosity and neutrino losses during MR explosion are represented.

The amounts of ejected mass ($\approx 0.13M_{\odot}$) and energy (6.1×10^{50} erg) are close to the corresponding values in the

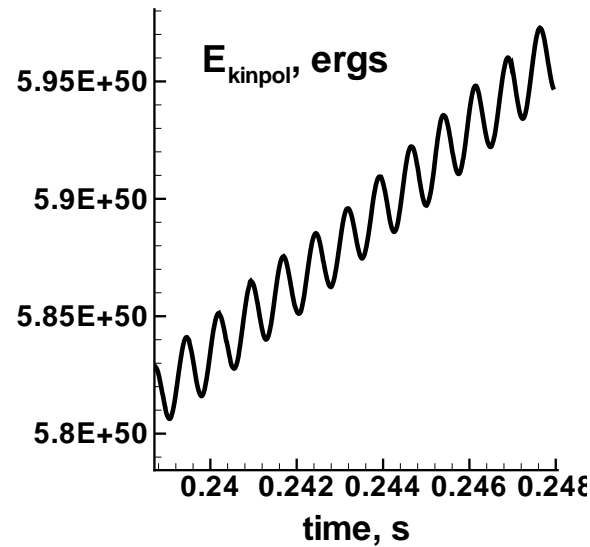


Figure 4. Zoomed part of the time evolution of the radial kinetic energy (Fig. 3) during MR explosion.

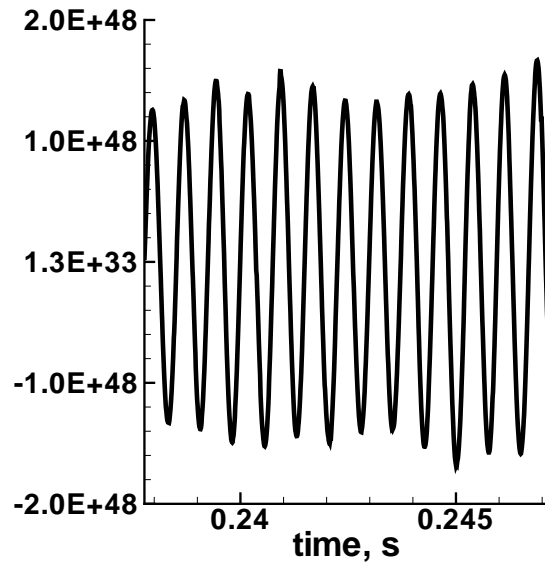


Figure 5. The time evolution of the kinetic energy of the core only during MR explosion.

case of MR supernova explosion with the initial quadrupole-like magnetic field. The plots of the time evolution of the ejected mass and energy for the dipole field are represented at Fig.8 and Fig.9.

The time evolution of the velocity field and temperature is represented in Figs.10 and 11. At the upper plot of the Fig.10 a zoom of the central part of the velocity field is represented. The shape of the supernova MHD shock is not spherical. Near z axis a protojet is forming. At the developed stages of MR explosion the shape of the shock front becomes more spherical, while the plot for the time evolution of the

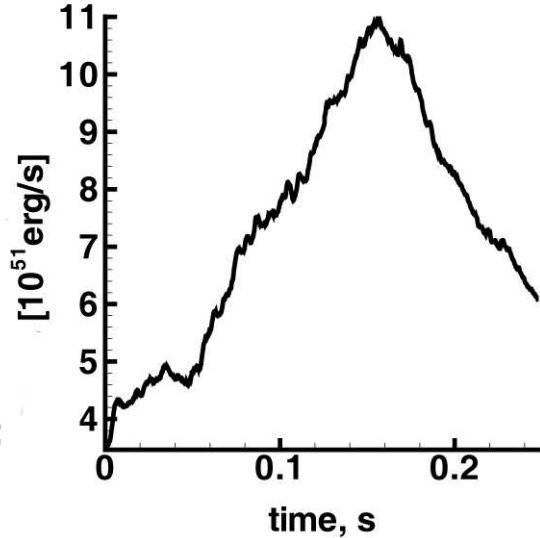


Figure 6. Time dependence of the neutrino luminosity $\int_0^{M_{\text{core}}} F(\rho, T) dm$ during MR explosion.

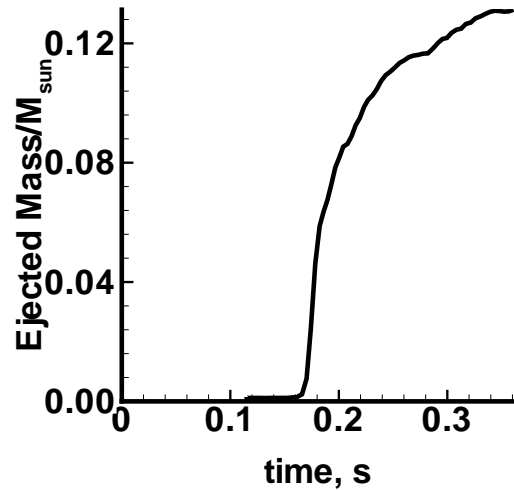


Figure 8. Time evolution of the ejected mass during MR explosion.

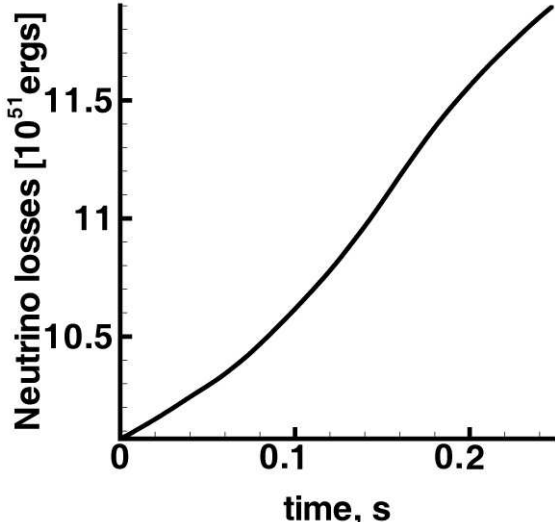


Figure 7. Time dependence of the neutrino losses during MR explosion.

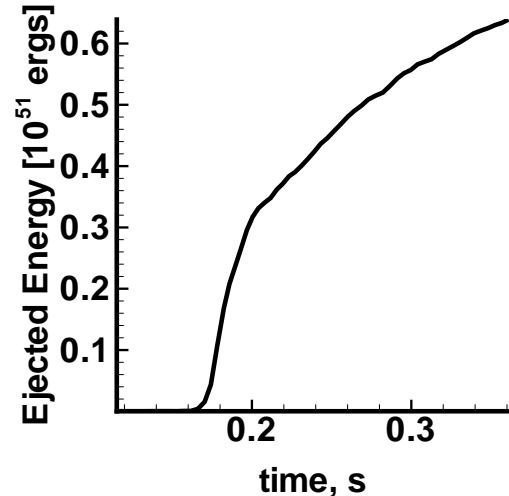


Figure 9. Time evolution of the ejected energy during MR explosion.

specific angular momentum Fig.12 shows that the angular momentum is extracted mainly along the axis of rotation z .

A development of the supernova shock leads to formation of a mildly collimated protojet. This protojet could be collimated stronger during passing through the vast envelope of the star and formation of the funnel flow.

As we have shown in the paper Ardeljan et al. (2005) the MR mechanism with the initial quadrupole-like magnetic field leads to the explosion which develops preferably near the equatorial plane. The shape of the MR explosion qualitatively depends on the initial configuration of

the magnetic field. The magnetic field with a pure dipole or quadrupole types of symmetry in the star is a simplification. In reality the structure of the magnetic field could be much more complicated what means that the resulting shapes of the MR supernova explosion could be rather different.

4.2 Appearance of the magnetorotational instability (MRI) in 2-D picture

It was shown in 1D simulations of MR supernova explosion Ardelyan et al. (1979) that the generated toroidal magnetic field is growing linearly with the time. Our recent 2D MR supernova simulations with the quadrupole-like initial magnetic field (Ardeljan et al. (2005)) have shown that, after

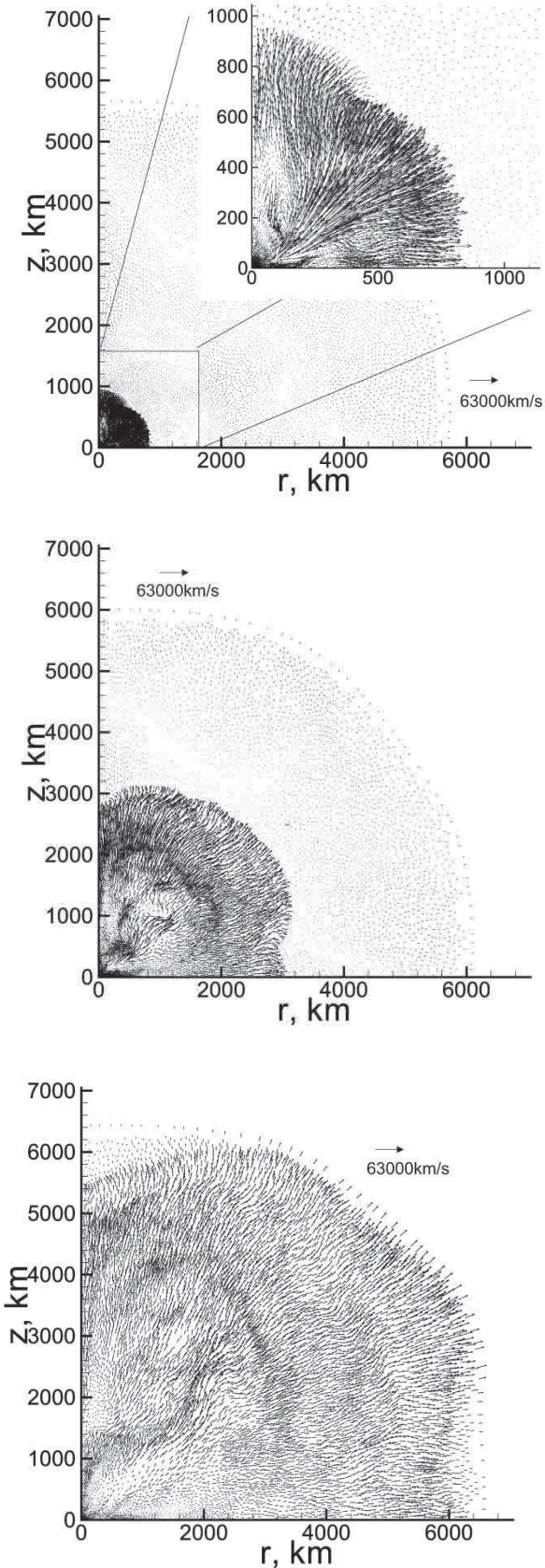


Figure 10. Time evolution of the velocity field for time moments $t = 0.075s, 0.1s, 0.25s$

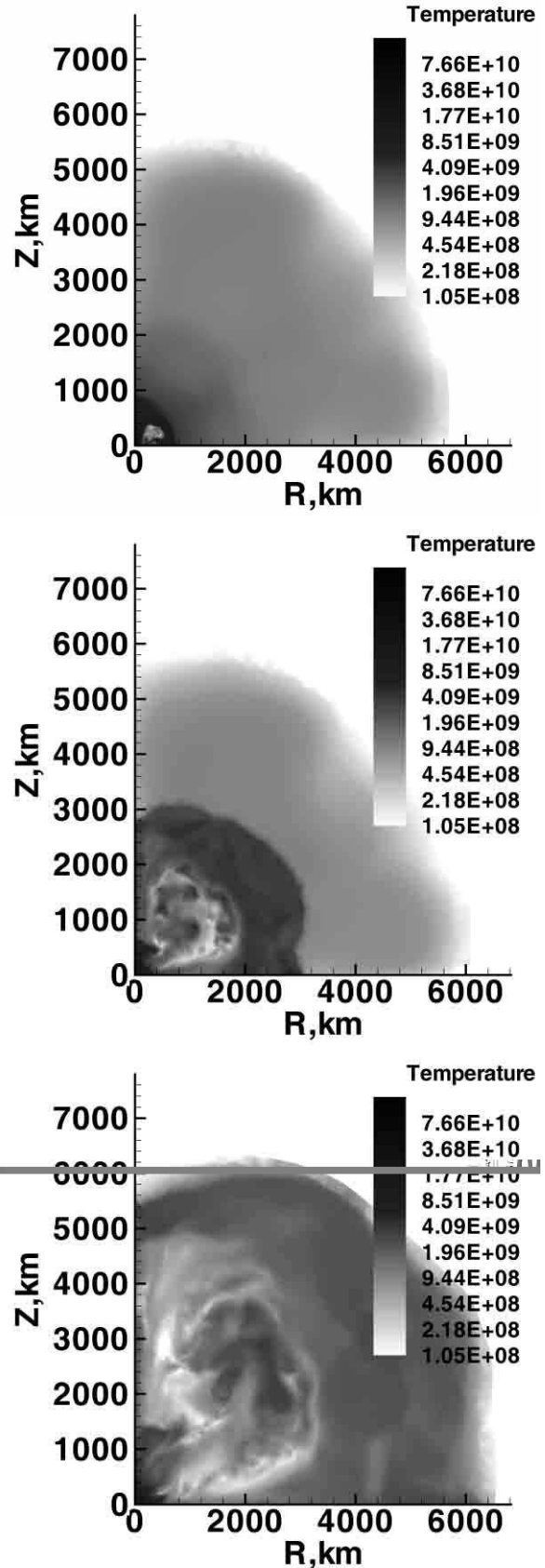


Figure 11. Time evolution of the temperature (in K) for time moments $t = 0.075s, 0.1s, 0.25s$.

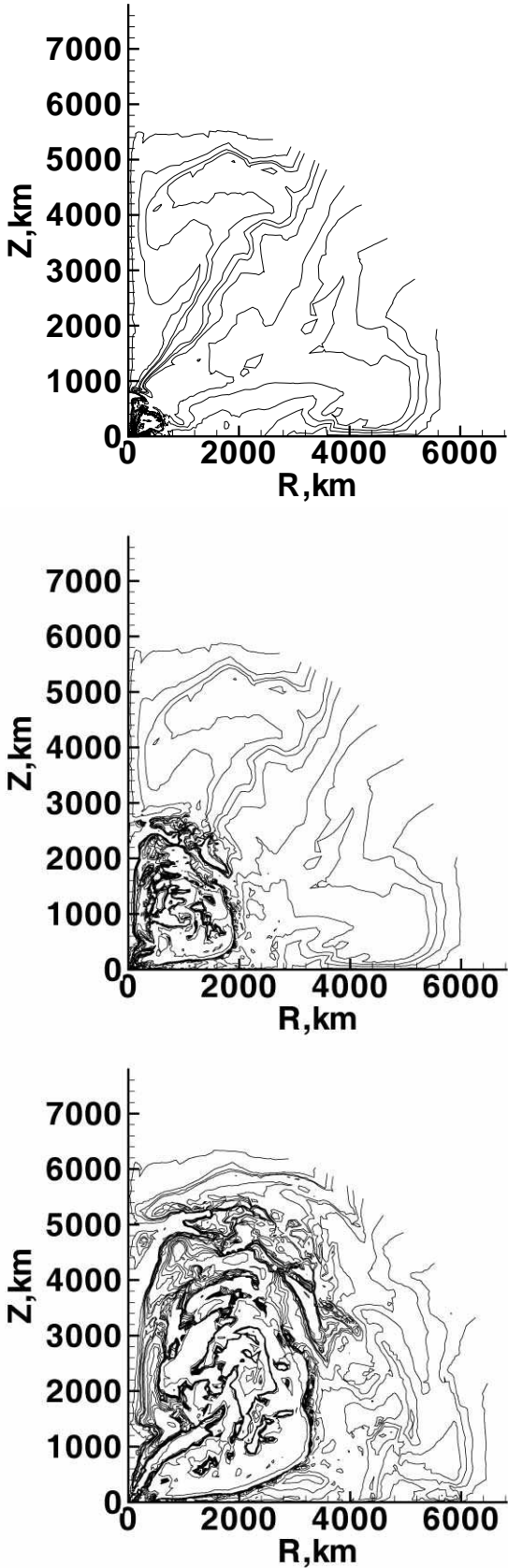


Figure 12. Time evolution of the specific angular momentum $v_\varphi r$ for time moments $t = 0.075s, 0.1s, 0.25s$.

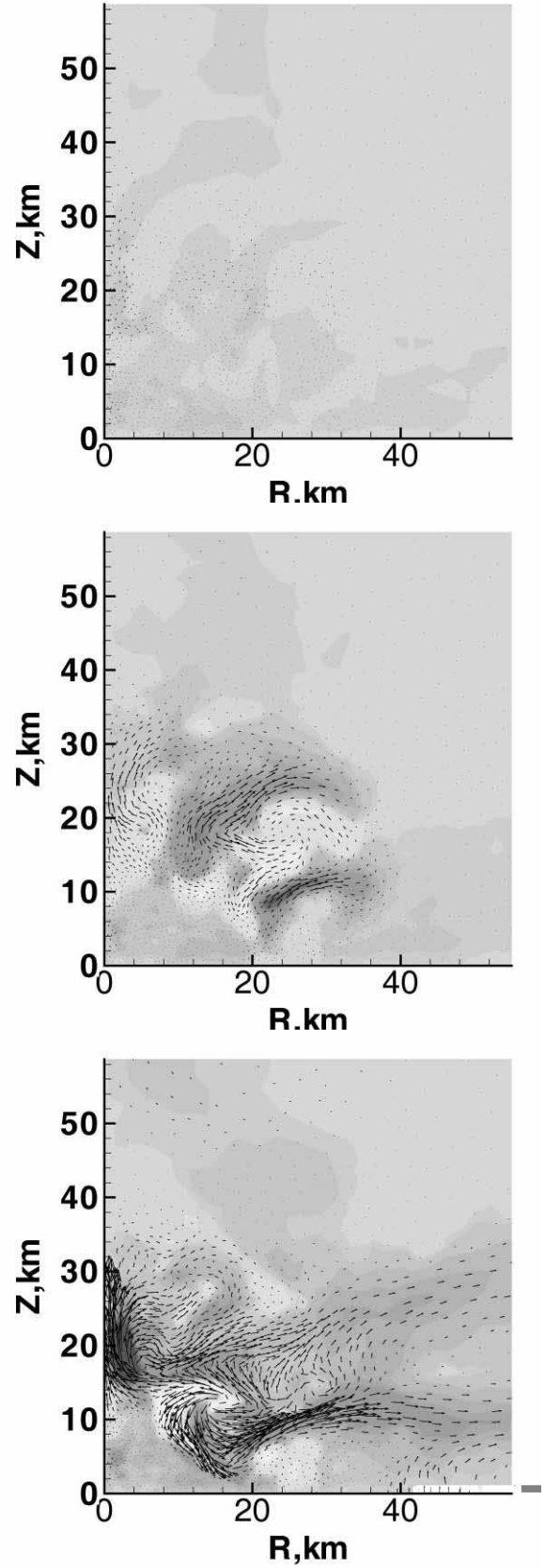


Figure 13. The MRI development for time moments $t = 0.0045, 0.018, 0.042s$. Gray scale is the toroidal field H_φ levels. Arrows show a direction and strength of the poloidal magnetic field H_r, H_z .

about 100 rotational periods of the central core, its linear growth changes to the exponential one, and the poloidal components also start to grow exponentially. The reason for that exponential growth is an onset of the variant of MRI, which was investigated by Tayler (1973). The qualitative explanation of MRI development for the MR supernova in 2D case was given by Ardeljan et al. (2005). Appearance of the MRI significantly reduces the evolution time of the MR supernova explosion. The picture of the MRI development in the present simulations is represented in Fig.13.

Let us define α as a ratio between the magnetic E_{mag0} and gravitational E_{grav0} energies at the moment of "turning on" of the magnetic field. It was found in 1D simulations that the time of the field amplification until the MR explosion, which is equal approximately to the time of the whole explosion t_{expl} , depends on α as $t_{expl} \sim \frac{1}{\sqrt{\alpha}}$. The results of 2-D MR supernova simulations with the initial quadrupole-like magnetic field have been represented in the paper by Moiseenko et al. (2004) for a wide range of variation of $\alpha = 10^{-2} \div 10^{-12}$. It was found, that for $\alpha < \sim 10^{-4}$ the growth of t_{expl} with decreasing α is becoming much slower, and may be well approximated by a logarithmic formula $t_{expl} \sim |\log \alpha|$ for small $\alpha \ll 1$. In the case of the dipole-like initial magnetic field we have made simulations for the same range of variation of the α parameter, and have found a similar dependence which is represented in Fig.14.

The logarithmic functional dependence at very small α has a simple qualitative explanation. First, we should have in mind, that the development of MRI starts at $t = t_{mri}$, approximately at the same moment for *all* initial values of the magnetic field. The MRI development begins in the part of the star, where the ratio of the toroidal and poloidal magnetic fields reaches a definite value $f \sim$ few tens, what happens after about 100 rotational periods of the inner core. In another words, the time of the field growth until the beginning of MRI t_{mri} does not depend on α , if α is small enough. At larger α the explosion starts before the beginning of MRI.

Second, we should take into account that MR explosion happens approximately at the same ratio $F < 1$ of the magnetic E_{mag} and internal E_{int} (gravitational E_{grav}) energies of the star, also for all α , $E_{magE} = F E_{grav}$. The magnetic energy E_{mag} is growing exponentially with time during MRI development at $t > t_{mri}$,

$$\frac{E_{mag}}{fE_{mag0}} = \exp[\gamma_m(t - t_{mri})], \quad (17)$$

where γ_m is an increment of the MRI instability. Therefore, the time between the the start of MRI, until the moment of the explosion t_{expl} , is growing logarithmically with decreasing α

$$\begin{aligned} t_{expl} - t_{mri} &= \frac{1}{\gamma_m} \log \frac{E_{magE}}{fE_{mag0}} = \frac{1}{\gamma_m} \log \frac{F E_{grav}}{f E_{mag0}} \\ &\approx \frac{1}{\gamma_m} \log \frac{F E_{grav0}}{f E_{mag0}} = \frac{1}{\gamma_m} \left(\log \frac{F}{f} - \log \alpha \right). \end{aligned} \quad (18)$$

Here it was taken into account that a relative change of the gravitational energy of the star during MagnetoRotational Explosion (MRE) is rather small, and $E_{grav}(t) \approx E_{grav0}$. At larger α the MRE happens before MRI instability begins, $t_{expl} < t_{mri}$, with $t_{expl} \sim 1/\sqrt{\alpha}$, and for small α , when $t_{expl} >> t_{mri}$, the explosion time is growing logarithmically.

This qualitative explanation is valid if the explosion happens during a linear stage of the MRI development, and the exponential growth of the magnetic energy. On this stage the magnetic field is growing exponentially with the increment roughly defined by the values of the configuration at the beginning of instability. When the magnetic field energy roughly approaches the rotational energy of the star, its growth is stopped, resulting in nonlinear saturation of MRI. Our numerical simulations have shown, that it is really the case, and the explosion occurs before the nonlinear saturation of MRI.

4.3 Influence of numerical dissipation, and magnetic field reconnection

We have done MR supernova explosion simulations with the initial dipole-like magnetic field (Fig.1) at a different number of knots in our triangular grid, starting from 1500 up to 18000 knots. We have found that the moment of the onset of the MRI depends visibly on the number of grid points. The less knots we have in the grid, the longer time it takes for starting the MRI. We have found that the results of the simulations (namely the time of the development of the MR supernova explosion) do not change when the total number of the knots N_n exceeds 15000. The results of the simulations described here are obtained with the grid containing about 15000 knots. The dependence (converging) of the time of the explosion t_{expl} on the number of knots has a pure numerical origin, and is connected with a numerical dissipation. Such dissipation has a stabilizing influence on the MRI, and its onset is shifted to larger values of f - the ratio of the toroidal and poloidal magnetic fields. Therefore, the total time of MRE is increasing with decreasing of the number of knots, due to increasing of the time t_{mri} . Numerical dissipation influence also on the field growth during MRI development, decreasing the increment γ_m , giving the same effect. As follows from our simulations the influence of the numerical viscosity becomes unimportant at $N_n \geq 15000$, when the time of viscous (numerical) dissipation starts to exceed all characteristic times of MR explosion.

In the simulations we supposed that the matter of the star has infinite conductivity, although in reality the conductivity is finite. In the case of a finite conductivity and chaotic structure of the magnetic field the reconnection of the magnetic field could be important, leading to a real physical dissipation.

The theory of the magnetic field reconnection is not complete up to now. To analyze the importance of the magnetic field reconnection in MRE, let us estimate (at least roughly) a characteristic time for this process. The growth of the magnetic field is accompanied by appearance of the chaotic small-scale structure of the magnetic field. If the characteristic reconnection time in smaller scales is comparable with characteristic time $\sim 1/\gamma_m$ of the magnetic field amplification due to MRI action, then reconnection could lead to a delay in the magnetic field growth, and hence could decrease the efficiency of MR explosion.

For the estimation of the characteristic time for the magnetic field reconnection we use the formula for the reconnection time of the quickest - Petschek-type reconnection (Priest & Soward (1976), Galeev et al. (1979)):

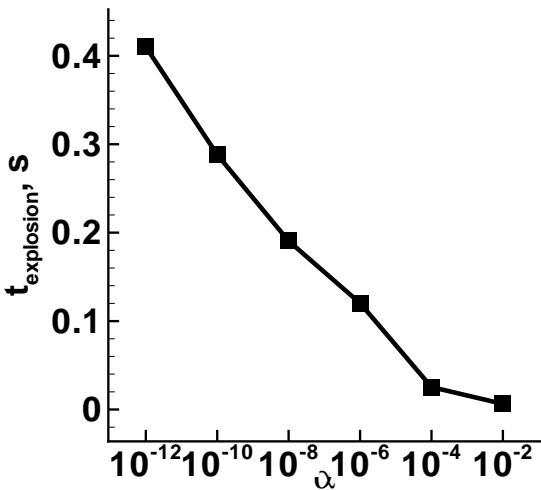


Figure 14. The dependence of the time evolution of the MR explosion on $\alpha = \frac{E_{\text{mag}}}{E_{\text{grav}}}$ for the case of the initial dipole-like magnetic field.

$$\tau_{\text{reconn}} = \frac{4(\ln(\text{Re}_m) + 0.74)}{\pi v_A l^{-1}}, \quad (19)$$

where $v_A = H/(4\pi\rho)^{1/2}$ is the Alfvén speed, $\text{Re}_m = 4\pi\sigma u l/c^2$ is the magnetic Reynolds number, l is the length, u is the velocity, ρ is the density, σ is the microscopic plasma conductivity, c is the light speed. In the region where the MRI is developing we have the following parameters: $u = 0.2 \cdot 10^{10}$ cm/s, $l = 10^5$ cm, $\rho = 7 \cdot 10^{12}$ g/cm³, $H = 0.17 \cdot 10^{14}$ G.

The plasma conductivity due to binary collisions σ is defined as (see e.g. Krall & Trivelpiece (1973))

$$\sigma = \frac{3m_e}{(16\sqrt{\pi})Ze^2\ln\Lambda} \left(\frac{2\alpha T}{m_e} \right)^{3/2}, \quad (20)$$

where $m_e = 9.1 \cdot 10^{-28}$ g is the electron mass, $\alpha = 1.38 \cdot 10^{-16}$ erg K⁻¹ is the Boltzmann constant, $e = 4.8 \cdot 10^{-10}$ is the electron charge, $Z = 27$ is the ion charge, $\ln\Lambda = 10$ is the Coulomb logarithm, $T = 10^{11}$ K is the temperature. The above expression gives the conductivity of electrons in a non-relativistic, non-degenerate plasma. Relativity may be taken approximately by substituting the light speed c^3 instead of the expression in brackets in (20), and increasing the electron mass in the numerator by relativistic factor $\gamma \approx 20$. Substituting all these data in formula (20) we find that conductivity is $\sigma \approx 8 \cdot 10^{20}$ s⁻¹. Note, the degeneracy of the electrons increase its conductivity, so this estimation may be considered as a lower limit for σ . The magnetic Reynolds number in our case is $\text{Re}_m \approx 10^{15}$. Substituting these data into the formula (19) we find the absolute lower limit for the characteristic reconnection time as

$$\tau_{\text{reconn}} \approx 5 \text{ s}$$

Our numerical simulations show that the characteristic time of the development of MRI is much smaller (~ 10 times) than the characteristic reconnection time. We can conclude

that the reconnection processes will not suppress magnetic field amplification and hence MR supernova explosion. The formula (19) for the characteristic time of the reconnection used here for the Petschek-type reconnection is the lower limit for the reconnection time. We can not assert that this type of the reconnection will be realized in the case of MR supernova mechanism while in the case of the realization of any other reconnection model the reconnection time will be even larger.

5 DISCUSSION

The results of the 2D numerical simulations of the MR supernova explosion with the initial dipole-like magnetic field have shown that MR supernova explosion is sensitive to the magnetic field configuration. MR supernova explosion with the initial quadrupole-like magnetic field develops mainly near the equatorial plane. In the case of the dipole-like magnetic significant part of the ejected matter obtains a velocity along the rotational axis. The total energy of the explosion in the MR mechanism does not depend significantly on the topology of the initial magnetic field. The explosion energy for quadrupole-like magnetic field is approximately equal to $0.61 \cdot 10^{51}$ erg Ardeljan et al. (2005), and for the dipole-like magnetic field its value is about $E_{\text{ejected}} \approx 0.5 \cdot 10^{51}$ erg. The amount of the ejected mass is approximately the same in both cases $M_{\text{ejected}} \approx 0.14M_{\odot}$. Comparison of the explosion times for the dipole-like and the quadrupole-like fields of the same initial magnetic energy, shows that in the quadrupole case the explosion is developing faster. The time of the explosion for the $\alpha = 10^{-6}$ is about ~ 0.12 s in the dipole case, and is about ~ 0.06 s in the case of the quadrupole.

In both cases we have done 2D simulations in a wide range of the initial magnetic field strength. The parameter α (the ratio between the initial magnetic energy and the gravitational energy of the star at the moment of "turning on" of the magnetic field) was chosen as

$$\alpha = \frac{E_{\text{mag}0}}{|E_{\text{gr}}|} = 10^{-2} \div 10^{-12}. \quad (21)$$

Comparison of the results of 1D simulations from Ardelyan et al. (1979), with a dependence of the MR explosion time on α as

$$t_{\text{expl}} \sim \frac{1}{\sqrt{\alpha}}, \quad (22)$$

with corresponding 2D results (Fig.14), shows a qualitative difference between them. The reason is a development of the MRI in 2D-case, which reduces drastically the MR explosion time t_{expl} . For the values of $\alpha > \sim 10^{-4}$ the dependence (22) holds approximately, while for smaller α values the MR explosion time depends on α in the following way:

$$t_{\text{expl}} \sim |\log \alpha|. \quad (23)$$

The axial protojet forming in our simulations is not narrow, while propagating through the envelope of the massive star this protojet could be collimated, or suffer mass entrainment and deceleration.

The collapse does not lead to strong amplification of the toroidal field, because its time in the central parts is comparable with rotation time. Besides, the initial configuration

is probably stable against MHD instabilities and (in reality) contains both parts, toroidal and poloidal, of the magnetic field. The relation between these components, and details of the initial angular velocity distribution (uniform in our case) may lead to different situations, when MRI starts to develop during the collapse, or after many rotational periods of the new born neutron star. Here we investigate the second case, as the initial step to the problem. The time separation of the hydrodynamic collapse from MRI and MRE helped us to understand the physical picture of MRI development, and to obtain the estimations for the energy production in MRE.

We plan to extend our calculations to a more realistic case when magnetic field will be included at the very beginning of the collapse. We expect to obtain more complicated picture of magnetohydrodynamical processes, which should not influence strongly on the energy production, which depend mainly on the initial rotational energy and angular velocity distribution.

In the paper by Sawai et al. (2005) a similar problem with rather strong initial magnetic field was simulated, and, contrary to our results, the authors did not find the development of MRI. Their simulations of the supernova explosion with weaker magnetic field did not lead to the development of MRI either and hence they did not get supernova explosion for a weak initial magnetic field. The authors of the Sawai et al. (2005) claim that MRI did not develop in their simulations due to the insufficient spatial resolution. The absence of the MRI in their calculations most probably is connected with a rather large numerical viscosity of the numerical scheme they used. The numerical viscosity of the simulations depends on characteristic size of the mesh. The bigger is the size of the cell the larger is the numerical viscosity. In the section 4.3 we have discussed the change of the MRI appearing time moment in dependence of the spatial resolution of our grid. In the case when the spatial resolution of the grid is very rough we probably do not get MRI in the case of application of our numerical method also.

It is known from the observations that the shapes of core collapse supernovae are different. From our simulations it follows that MR supernova explosion arises after development of the MRI. The development of the MRI is a stochastic process and hence the resulting shape of the supernova can vary. We may conclude that MR supernova explosion mechanism can lead to different shape of the supernova. It is important to point out that MR mechanism of supernova explosion leads always to asymmetrical outbursts.

The simulations of the MR supernova explosions for the initial quadrupole-like magnetic field described in the paper by Ardeljan et al. (2005) and MR supernova explosion described in current paper are restricted by the symmetry to the equatorial plane. While in reality this symmetry can be violated due to the MRI, simultaneous presence of the initial dipole and quadrupole -like magnetic field (Wang et al. (1992)) and initial toroidal magnetic field (Bisnovatyi-Kogan & Moiseenko (1992)). The violation of the symmetry could lead to the kick effect and formation of rapidly moving radio pulsars.

When rotational and magnetic axes do not coincide the whole picture of the explosion process is three dimensional. Nevertheless, the magnetic field twisting happens always around the rotational axis, so we may expect the kick ve-

locity of the neutron star be strongly correlated with its spin direction, also due to the anisotropy of the neutrino flux Bisnovatyi-Kogan (1993). Simultaneously, because of the stochastic nature of MRI, the level of the anisotropy should be strongly variable, leading to a large spreading in the the neutron star velocities. This prediction of MR explosion differs from the models with a powerful neutrino convection, where arbitrary direction of the kick velocity is expected (Burrows et al. (1995), Janka & Müller (1995)). Recent analysis of observations of pulsars (Johnston et al. (2005)) shows, that rotation and velocity vectors of pulsars are aligned, as it is predicted by the MR supernova mechanism. The alignment of the vectors can be violated in the case when supernova explodes in a binary system.

ACKNOWLEDGMENTS

The authors would like to thank RFBR in the frame of the grant No. 05-02-17697-a and the program "Nonstationary phenomena in astronomy" for the partial support of this work. We would like to thank Andrew Sadovskii for useful discussion and anonymous referee for careful reading of the article and useful comments.

REFERENCES

- Akiyama S., Wheeler J.C., Meier D.L., Lichtenstadt I., 2003, ApJ, 584, 954
- Ardeljan N.V., Bisnovatyi-Kogan G.S., Kosmachevskii K.V., Moiseenko S.G., 1996, A&A Supl.Ser., 115, 573
- Ardeljan N.V., Bisnovatyi-Kogan G.S., Kosmachevskii K.V., Moiseenko S.G., 2004, Astrophys., 47, 1
- Ardeljan N.V., Bisnovatyi-Kogan G.S., Moiseenko S.G., 2000, A&A, 355, 1181
- Ardeljan N.V., Bisnovatyi-Kogan G.S., Moiseenko S.G., 2005, MNRAS, 359, 333
- Ardelyan N.V., Bisnovatyi-Kogan G.S., Popov Yu.P., 1979, Astron. Zh. 56, 1244
- Ardelyan N.V., Bisnovatyi-Kogan G.S., Popov Yu.P., Chernigovsky S.V., 1987a, Astron. Zh. 64, 761 (Soviet Astronomy, 1987, 31, 398)
- Ardeljan N.V., Kosmachevskii K.V. 1995, Computational mathematics and modeling, 6, 209
- Ardeljan N.V., Kosmachevskii K.V., Chernigovskii S.V., 1987, Problems of construction and research of conservative difference schemes for magneto-gas-dynamics, MSU, Moscow (in Russian)
- Baym G., Pethick C., Sutherland P., 1971, ApJ, 170, 299
- Bisnovatyi-Kogan G.S., 1970, Astron. Zh. 47, 813 (Soviet Astronomy, 1971, 14, 652)
- Bisnovatyi-Kogan G.S. 1993, Astron. Ap. Transact. 3, 287
- Bisnovatyi-Kogan G.S., Moiseenko S.G. 1992, Astron. Zh. 69, 563 (Soviet Astronomy, 1992, 36, 285)
- Bisnovatyi-Kogan G.S., Popov Yu.P., Samokhin A.A., 1976, ApSS, 41, 321
- Bisnovatyi-Kogan G.S., Tutukov A.V., 2004, Astronomy Reports, 49, 724
- Burrows A., Hayes J., Fryxell B.A. 1995, ApJ, 450, 830
- Burrows A., Livne E., Dessart L., Ott C., Murphy J., 2006, ApJ, 640, 878

Ivanova L.N., Imshennik V.S., Nadezhin D.K., 1969, *Nauchn. Inform. Astron. Sov. Akad. Nauk SSSR (Sci. Inf. of the Astr. Council of the Acad. Sci. USSR)*, 13, 3

Galeev A.A., Rosner R., Vaiana G.S., 1979, *ApJ*, 229, 318

Janka H.-T., Müller E. 1995, *ApJ Lett.* 448, L109

Johnston S., Hobbs G., Vigeland S., Kramer M., Weisberg J.M., Lyne A.G., 2005, *astro-ph/0510260*

Kotate K., Yamada S., Sato K., 2003, *ApJ*, 595, 304

Kotate K., Sawai H., Yamada S., Sato K., 2004, *ApJ*, 608, 391

Krall N.A., Trivelpiece A.W. (1973) *Principles of plasma physics*, McGraw-Hill, New York

LeBlanc J.M., Wilson J.R., 1970, *ApJ*, 161, 541

Malone R.C., Johnson M.B., Bethe H.A., 1975, *ApJ*, 199, 741

Meier D.L., Epstein R.I., Arnett W.D., & Schramm D.N. 1976, *ApJ*, 204, 869

Moiseenko S.G., Bisnovatyi-Kogan G.S., Ardeljan N.V., 2004, *Magnetorotational supernova simulations*, in "1604-2004 Supernovae as Cosmological Lighthouses" (San Francisco: ASP), (in press), (*astro-ph/0410330*)

Müller E., Hillebrandt W., 1979, *A&A*, 80, 147

Ohnishi N., 1983, *Tech. Rep. Inst. At. En. Kyoto Univ.*, No.198

Priest E.R., Soward A.M., 1983, in *Proc. IAU Symposium 71, Basic Mechanisms of Solar activity*, ed. V.Bumba and J.Klecze (Dordrecht: Reidel), p.353

Sawai H., Kotake K., Yamada S., 2005, *ApJ*, 631, 446

Schinder P.J., Schramm D.N., Wiita P.J., Margolis S.H., Tubbs D.L., 1987, *ApJ*, 313, 531

Spruit H.C., 2002, *A&A*, 381, 923

Symbalisty E.M.D., 1984, *ApJ*, 285, 729

Taylor R.J., 1973, *MNRAS*, 161, 365

Wang, J. C. L., Sukanen, M. E., Lovelace, R. V. E., 1992, *ApJ*, 390, 46

Yamada S., Sawai H., 2004, *ApJ*, 608, 907

Yamasaki T., Yamada S., 2005, *ApJ*, 623, 1000

This paper has been typeset from a *TeX/ L^AT_EX* file prepared by the author.